

# **Analytical Analysis of the Sail-Boom Subsystem and Membrane Deployment in Large Scale Satellite Design**

*Yasmina Elmore*

# Contents

<b>1. Configuration design</b>	<b>2</b>
1.1 General concept . . . . .	3
1.2 Preliminary Design objectives . . . . .	3
1.3 Requirements . . . . .	4
<b>2. Sail-Boom Subsystem (SBS) Design</b>	<b>5</b>
2.1 General design overview and dimensions . . . . .	6
2.2 Bi-CTM booms . . . . .	6
2.3 The SBS deploying mechanism . . . . .	7
2.4 Miura-Ori membrane folding . . . . .	10
<b>3. Packaged dimensions</b>	<b>14</b>
3.1 Boom thickness for equal and opposite sense coiling . . . . .	15
3.2 Minimum coiling radius $r$ . . . . .	16
3.3 Outer coiling radius $r_o$ . . . . .	16
3.4 Dimensions of the stowed membrane . . . . .	17
3.5 Expression of the flattened length of the Bi-CTM booms . . . . .	17
3.6 Back-to-the envelope calculations . . . . .	18
<b>4. Geometry in the fully deployed case</b>	<b>20</b>
4.1 Second momentum of area of the Bi-CTM booms . . . . .	21
4.2 Impact of the material of the geometry of the Bi-CTM boom . . . . .	22
4.3 Fundamental frequency of the Bi-CTM boom . . . . .	23
<b>5. Design of the boom and the membrane</b>	<b>24</b>
5.1 Overall design of the Bi-CTM boom . . . . .	25
5.2 Preliminary design parameters : coiling radius $r$ and thickness $t$ . . . . .	25
5.3 Preliminary parameters design choice : $\theta$ . . . . .	26
5.4 Validation of the preliminary design parameter : $\theta$ . . . . .	27
5.5 Packaged dimensions of the membrane . . . . .	28
5.6 Algorithm . . . . .	29
<b>6. MATLAB Code</b>	<b>30</b>

# 1. Configuration design

## 1.1 General concept

This work introduces a Sail-Boom Subsystem (SBS) design for a square three-layer membrane sunshade with dimensions of  $20\text{ m} \times 20\text{ m}$ . The concept has three main assemblies:

1. the three-layer sunshade membrane, composed of  $50\text{ }\mu\text{m}$  thick Kapton coated with a  $100\text{ nm}$  aluminum layer
2. the deployment mechanism comprised of a SBS boom deploying mechanism and four Collapsible Tubular Mast (CTM) booms
3. the tensioning and support system, which maintains a spacing of  $10\text{ cm}$  between each membrane layer

This model is inspired from the Advanced Composite Solar Sail System (ACS3) SBS, designed by the National Aeronautics and Space Administration (NASA) and the German Aerospace Center (DLR). DLR has developed for SmallSat solar sailing and deploys a single layer sunshade of  $9\text{ m} \times 9\text{ m}$ . This design adjustments for larger satellite configurations and multiple membrane layers sunshades.

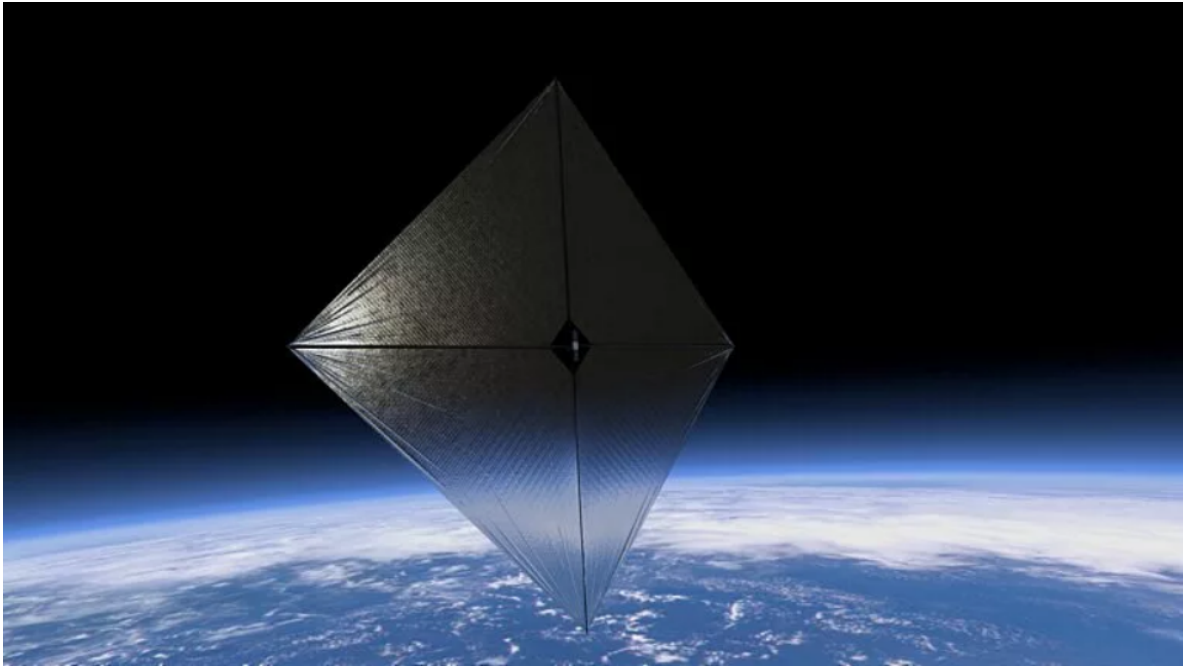


Figure 1: NASA ACS3 Solar Sail: Concept of the solar sail spacecraft in Earth orbit. *Image: NASA*

## 1.2 Preliminary Design objectives

This project is divided into two phases.

The first phase from September to December explores design and concept for the SBS in the context of a  $20 \times 20\text{ m}^2$  three-layer sunshade for a satellite. This phase follows a theoretical approach, inspired from the existing ACS3 model to propose viable deployment mechanisms. This initial phase will also result in a potential algorithm that can be used to determine the preliminary design parameters.

The second phase from January to March focuses on technology prototyping and demonstration of a design. It aims to construct the SBS at a more adapted scale for ground testing.

### **1.3 Requirements**

#### Sunshade Performance Requirements :

- $R_1$  : The sunshade subsystem membranes shall each have a deployed area of  $20 \text{ m} \times 20 \text{ m}$
- $R_2$  : The sunshade shall contain three layers
- $R_3$  : The sunshade membrane layers shall be made of  $50 \mu\text{m}$  thick Kapton coated with a  $100 \text{ nm}$  Aluminum layer
- $R_4$  : The sunshade layers shall have  $10 \text{ cm}$  nominal separation between each layer
- $R_5$  : The sunshade layers shall be separated from each other during operation

#### Mechanical Requirements :

- $R_6$  : The sunshade subsystem shall not have a mass less than  $200 \text{ kg}$
- $R_7$  : The deployable sunshade subsystem shall stow in a volume of  $0.5 \text{ m} \times 0.5 \text{ m} \times 0.3 \text{ m}$
- $R_8$  : The sunshade subsystem shall have a first mode frequency above  $0.1 \text{ Hz}$
- $R_9$  : The sunshade subsystem shall interface with a spacecraft bus of  $0.5 \text{ m} \times 0.5 \text{ m}$  in size located at its center

#### Mechanical Requirements :

- $R_{10}$  : The sunshade subsystem shall survive a thermal environment from  $-178^\circ < T < 150^\circ$
- $R_{11}$  : The sunshade subsystem shall prevent tears from spreading beyond  $2 \text{ m} \times 2 \text{ m}$  area
- $R_{12}$  : The sunshade layers shall be vented in the stowed configuration

## **2. Sail-Boom Subsystem (SBS) Design**

## 2.1 General design overview and dimensions

The conceptual SBS consists of three layers of membrane supported by four deployable composite booms that are actuated by an SBS deploying mechanism. The platform of the deployed conceptual design is shown in Figure 2. The dimensions of the fully deployed membrane are  $20\text{ m} \times 20\text{ m}$ , which means that the following expression can define the entire length of the deployed boom:

$$l = \sqrt{(20/2)^2 + (20/2)^2} \simeq 14.14\text{ m}$$

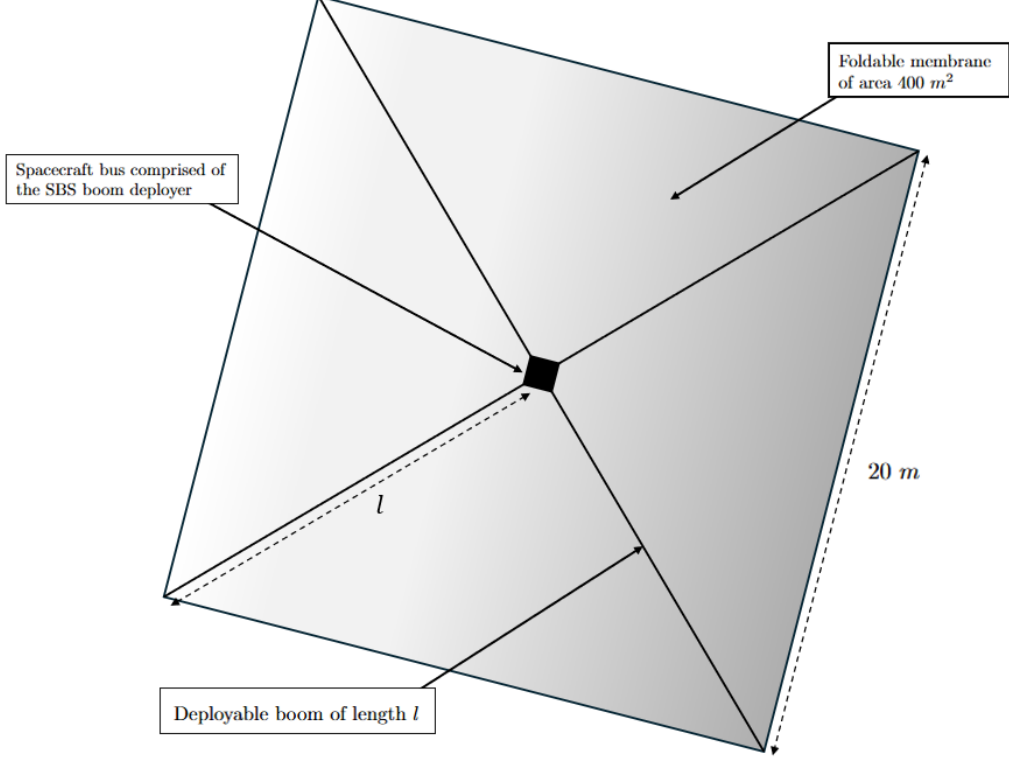


Figure 2: Overall conceptual design of the deployed SBS in Earth orbit

We also know that the sunshade subsystem shall interface with a spacecraft bus of size  $0.5\text{ m} \times 0.5\text{ m}$ , located at its center. This means that the SBS deploying mechanism boom system cannot exceed the dimensions of  $0.5\text{ m} \times 0.5\text{ m}$ .

## 2.2 Bi-CTM booms

The SBS design is comprised of four slit-tube Bi-stable Collapsible Tubular Mast (CTM) booms, which are booms developed during the Deployable Composite Booms (DCB) project and used in the ACS3 mission. These booms are designed using ultra-thin carbon fiber composite materials ensuring high strain curvature tolerance and high bending stiffness. They can be flattened and rolled around a spool for compact stowage with a high packaging efficiency, making them particularly suited for spacecraft limited storage volumes. Once deployed, they act as lightweight strong supports for the SBS that can be used solar sails system.

The Bi-CTM booms cross-section design allows them to sustain higher compression loads while minimizing a risk of buckling. These booms possess the property of high thermal stability, property interesting to limit thermal distortions of the SBS boom system in space environments. Furthermore, their lower material density reduce the payload constrains while still ensuring high stiffness. The key structural characteristics of the Bi-CTM booms in the ACS3 design are illustrated in Figure 12.

To meet our requirements, we will consider the Bi-CTM booms used in the ACS3 mission and propose design improvements, different material selections, and alternative dimensions to adapt them to our model better.



Figure 3: Key structural design of the CTM booms in the ACS3 mission

Each Bi-stable CTM booms is characterized by five different sections. The design of the Bi-CTM boom will be discussed later in the project in order to define the relevant preliminary design parameters used in order to manufacture of a boom that meets the requirement for a large-scale sunshade. A schematic and a cross-sectional view of the CTM boom are provided in Figure 8.

For the ASC3 design [Wil21], the geometry of the CTM booms is characterized by a total height of 65 mm (dimension  $h$ ) when flattened for coiling. Once deployed, the height turns around 50 mm and 33 mm in width. A schematic of the ACS3 boom cross-section is shown in Figure 5.

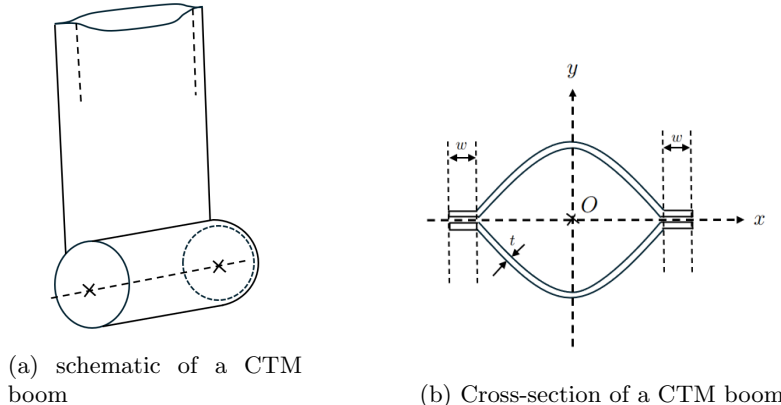


Figure 4: Dimensions and Geometry of a CTM boom

## 2.3 The SBS deploying mechanism

The SBS deploying mechanism is based on a "tape-puller" concept developed by the German Aerospace Center (DLR). The ACS3 design uses a 12U version of this deploying system. The ASC3 SBS concept is provided in Figure 6. The additional metallic tape spring helps in a better control of the Bi-CTM

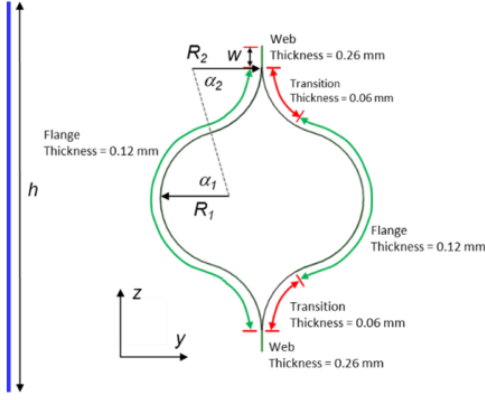


Figure 5: Cross sectional view of the ASC3 deployable Bi-CTM boom design [Wil21]

booms deployment through their motorized retraction. Those springs are co-wound with the composite booms in stowed configuration.

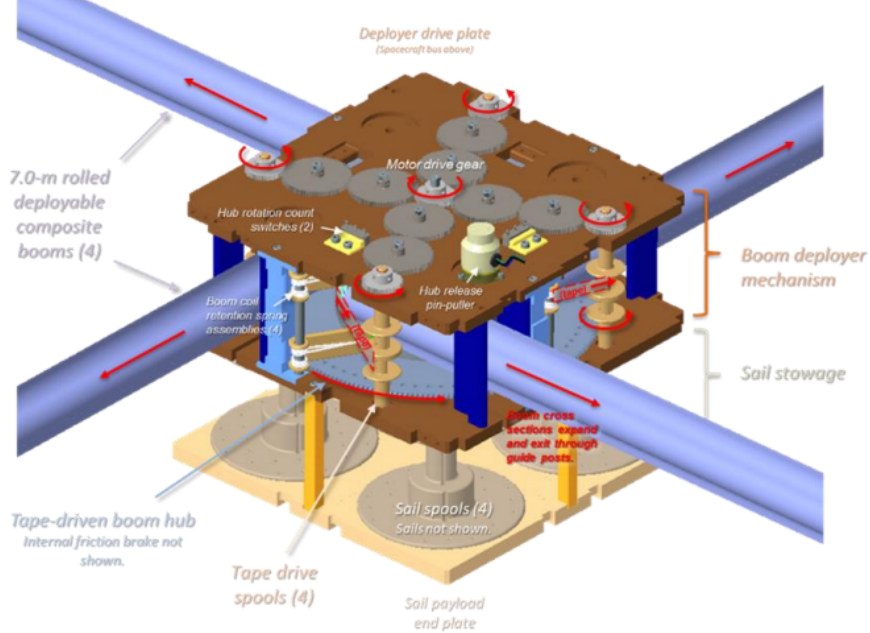


Figure 6: ASC3 Sail-Boom Subsystem deploying mechanism [Wil21]

The metallic tapes are made of ultra-thin, flexible, and durable stainless steel making them more resistance to plastic deformation. In the stowed configuration, the tapes are coiled alongside the composite booms, positioned on the outer surface of the boom coil, as shown in Figure 10. They apply pressure on the booms to ensure tight coiling around the boom spool, counteracting the booms' natural tendency to uncoil [SH21]. During deployment, the tapes are retracted by its own electrically controlled drive unit that are coordinated with the boom spool, ensuring high level control of the deployment process of the booms.

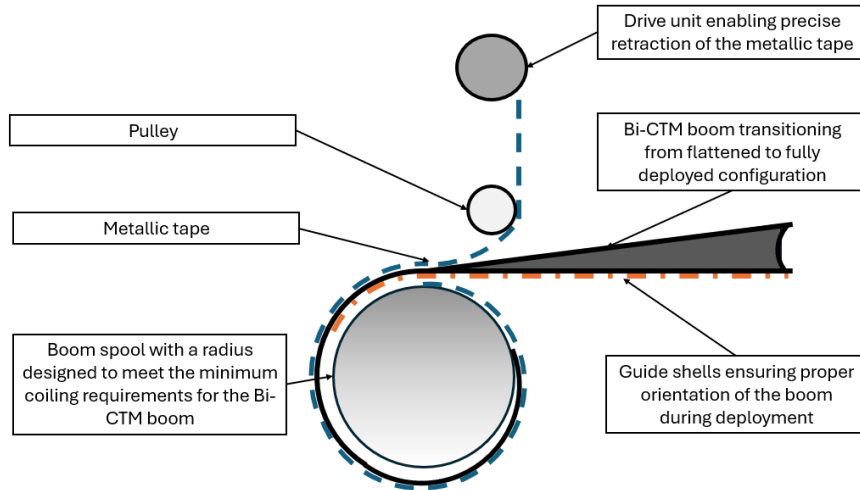
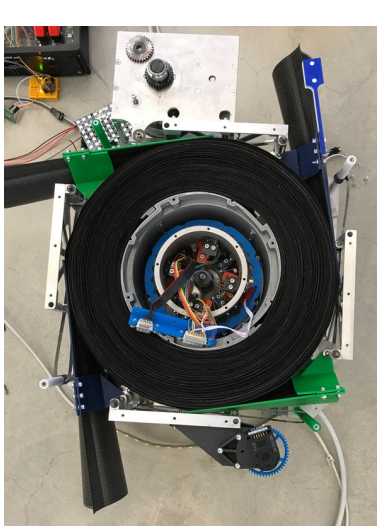
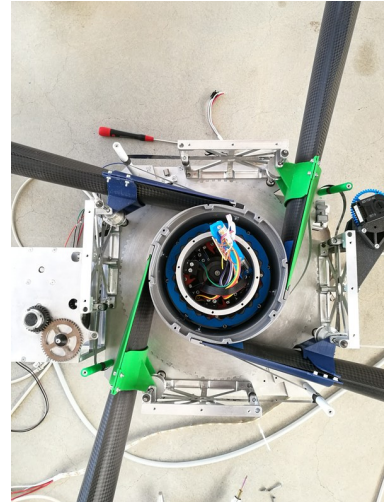


Figure 7: SBS tape-puller system for deploying the Bi-CTM booms, illustrated with a single CTM boom instead of four for clarity

This design prevents mechanical stress, jamming, and blossoming. It also ensures a smooth deployment of the booms.



(a) Fully stowed configuration of the booms [Cen21]



(b) Fully deployed configuration of the booms to support the solar sail structure [Cen21]

Figure 8: Illustration of the SBS deploying mechanism in its compact and deployed states. *Source: DLR*

## 2.4 Miura-Ori membrane folding

In the ACS3 solar sail design, the deployable structure is comprised of four triangular membranes, referred to as quadrants. These quadrants are made of 2.115 mm Al/PEN/Cr composite material and folded using parallel and wedge fold patterns. However, the quadrants do not provide shielding in certain parts of the ACS3 design for the telescope, which may be unsuitable for our requirements, as shown in Figure 9. In our design, we prioritize the protection of the telescope from direct solar radiation. To achieve this, we will use one square membrane with dimensions of  $20\text{ m} \times 20\text{ m}$ , folded using a specific pattern, that will be discussed in this section.

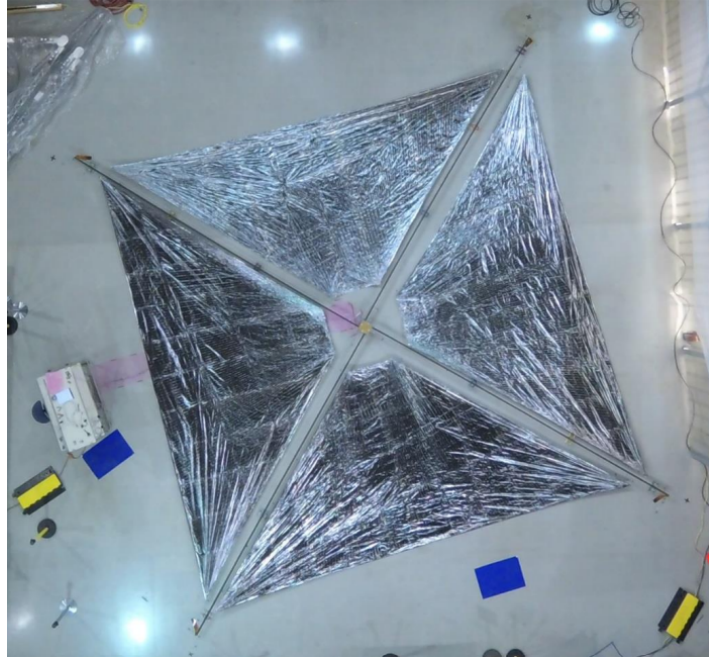


Figure 9: Fully deployed membrane highlighting the empty gaps between quadrants [Wil21]

For the folding methods, we will primarily focus on the Miura-Ori folding due to its compatibility with the SBS deploying mechanism. Indeed, we consider two main deployments of membranes : *sequential deployment*, such as the Z-fold, and *synchronous deployment*, such as the Miura-Ori folding that enables the membrane to unfold as a whole. The second configuration aligns well with the boom deploying mechanics.

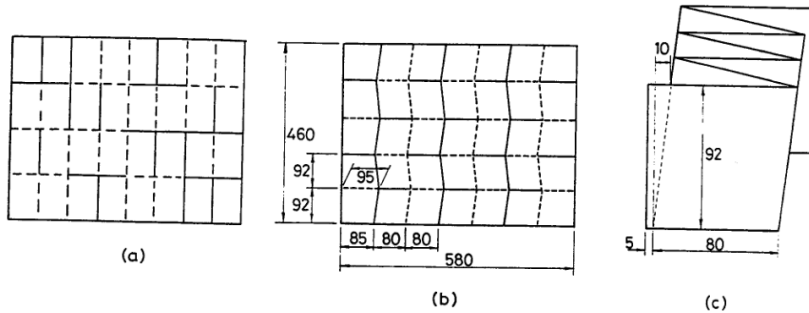
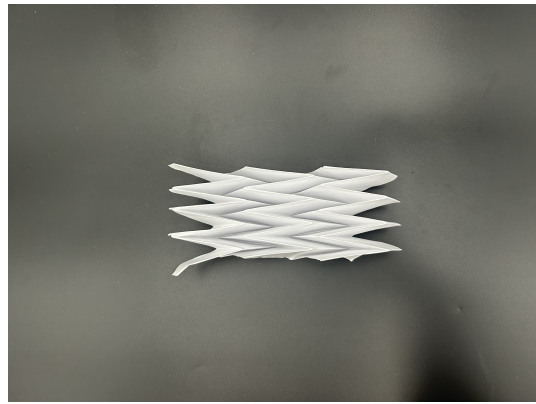


Figure 10: Fold Patterns Examples [GP92]: (a) Z-fold pattern; (b) Miura-Ori fold pattern when fully deployed; (c) Miura-Ori fold pattern when folded



(a) Fully folded membrane using Miura Ori fold pattern and about to be deployed



(b) Initial deployment step when the pattern starts unfolding



(c) Miura Ori folding partially expanded when the membrane is , showcasing the unfolding geometry



(d) Midway through deployment of the membrane



(e) Nearly fully deployed membrane showing Miura Ori pattern significantly expanded

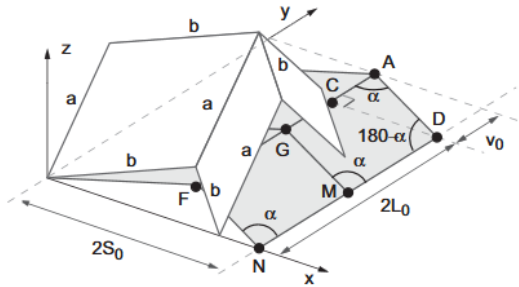


(f) Fully deployed membrane showing the Miura Ori pattern when fully expanded

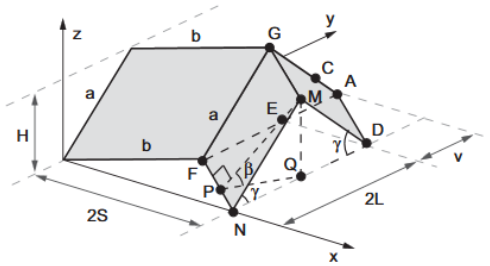
Figure 11: The sequence illustrates the deployment process of an in-house made membrane using paper and folded using Miura-Ori pattern showing the membrane synchronous deployment and demonstrating its efficient packaging.

For the crease pattern, the Miura-Ori folding is characterized by specific geometric parameters that is determined through a back-of-the-envelope calculation.

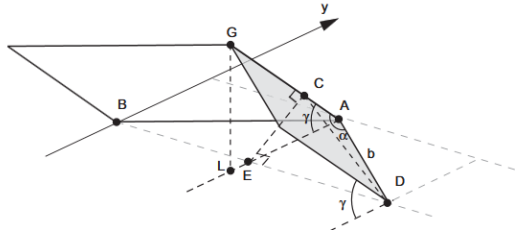
- $S, S_0$  (initial) width
- $L, L_0$  (initial) length
- $H$  height
- $\alpha$  the parallelogram internal angle
- $\beta$  the deployment angle
- $a$  and  $b$  the parallelogram dimensions
- $n^2$  the number of unit cells (composed of 4 parallelograms) in the concept



(a) Geometry of a unit cell highlighting the angle  $\alpha$   
[MP20]



(b) Geometry of a partially folded unit cell highlighting  
the angle  $\beta$  [MP20]



(c) Different of the geometry defined in (b) hightlighting  
the angle  $\gamma$  [MP20]

Figure 12: Geometry of a unit cell highlighting the different angles essential to define the deployment and packaging of the Miura-Ori pattern

From [MP20], we can define the ratios of the dimensions when the membrane is deploying over the initial dimensions (when the membrane is flattened), but they do not correspond to the packaged dimensions. For one unit cell, these ratios are given by:

$$H = a \sin(\alpha) \sin(\beta). \quad (1)$$

$$\frac{S}{S_0} = \frac{\cos(\beta)}{\cos(\alpha) \sqrt{1 + \tan^2(\alpha) \cos^2(\beta)}}, \quad (2)$$

$$\frac{L}{L_0} = \sqrt{1 - \sin^2(\alpha) \sin^2(\beta)}. \quad (3)$$

In the packaged configuration, the deployment angle approaches  $\beta = \frac{\pi}{2}$ , allowing us to determine the corresponding packaged dimensions. Specifically, the total packaged length  $L_p$  for  $n^2$  unit cells, which represents the stowed length of the folded membrane, is given by:

$$L_p = b + 2n \left( \frac{L}{L_0} \right) a = b + 2n \cos(\alpha) a. \quad (4)$$

Similarly, the packaged height  $H_p$ , corresponding to the total height of the stowed membrane, is given by:

$$H_p = a \sin(\alpha). \quad (5)$$

These expressions characterize the geometric constraints imposed by the Miura-Ori fold pattern when fully packaged and need to meet the constraints defined by requirement  $R_7$ . A detailed analysis of the folding dimensions that meet the stowage constraints will be presented in Section ??.

### **3. Packaged dimensions**

### 3.1 Boom thickness for equal and opposite sense coiling

Before analyzing the geometry of the CTM booms, we can first examine the coiling sense. There are two types of coiling: equal sense coiling and opposite sense coiling, as shown on Figure 13.

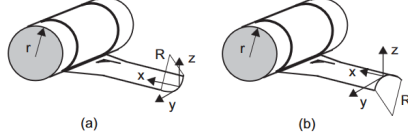


Figure 13: Booms coiling sense [MP20]: (a) Equal sense coiling; (b) opposite sense coiling

For opposite sense coiling, with a coiling radius  $r$ , we can derive an expression for the radius  $R$  of curvature of the tape spring, assuming that the material remains within the elastic domain [MP20]. The relationship between  $R$ , the yield strength  $\sigma_Y$ , and the thickness  $t$  of the tape spring is given by:

If :

$$\frac{r}{R} > 1$$

$$\frac{R}{t} = \frac{E}{2 \times \sigma^y(1 - \nu^2)} \times \frac{\nu + \frac{r}{R}}{\frac{r}{R}} \quad (6)$$

where  $E$  is the Young's modulus of the material and  $\sigma_Y$  is the yield strength of the material.

For equal sense coiling, the expression depends on Poisson's ratio  $\nu$  [MP20], which characterizes the material's lateral strain when subjected to axial stress. The tape's radius of curvature  $R$  for the equal sense coiling can be expressed as:

If :

$$\frac{1}{\nu} < \frac{r}{R}$$

$$\frac{R}{t} = \frac{E}{2 \times \sigma^y(1 - \nu^2)} \times \frac{-\nu + \frac{r}{R}}{\frac{r}{R}} \quad (7)$$

Else if :

$$1 < \frac{r}{R} < \frac{1}{\nu}$$

$$\frac{R}{t} = \frac{E}{2 \times \sigma^y(1 + \nu)} \times \frac{1 + \frac{r}{R}}{\frac{r}{R}} \quad (8)$$

For the flat surface, the thickness  $t$  can be related to the coiling radius  $r$  by the relation:

$$t = \frac{2r\sigma_y}{E} \quad (9)$$

### 3.2 Minimum coiling radius $r$

The minimum initial coiling radius  $r$  can be approximated using Euler-Bernoulli theory for thin sections and is defined by the material's modulus of elasticity in the boom axial direction  $\varepsilon_{y11}$  for a given thickness  $t$ . The modulus of elasticity  $E_{11}$  quantifies the maximum strain of the material to yield in the boom axial direction and represents the maximum stress for elastic coiling :

$$\varepsilon_{y11} = \frac{\sigma_{y11}}{E_{11}} = \frac{t}{2r}, \quad (10)$$

The maximum curvatures of any deployed Bi-CTM booms is defined by the ratio  $1/R$ . Prior to coil, the curved segment of the Bi-CTM booms need to be flattened. In order to keep the elastic property of the material, we need to consider and quantify the maximum strain to yield in the transverse direction. Thus, Eq. (10) in the transverse direction translates to:

$$\varepsilon_{y22} = \frac{\sigma_{y22}}{E_{22}} = \frac{t_{sh}}{2R}, \quad (11)$$

### 3.3 Outer coiling radius $r_o$

The outer radius of the coil  $r_o$  for a four Bi-CTM booms system can be estimated using the Archimedian spiral approximation [Fer17].

$$r_o = r + w \times nt(1 + \mu) \quad (12)$$

With :

- $n$  is the total number of booms coiled. In our configuration  $n = 8$
- $\mu$  is the packaging efficiency. In our configuration  $\mu = 0.25$
- $t$  is the thickness of the boom
- $r$  is the minimum coiling radius, or inner coiling radius

The total number of wraps  $w$  is estimated using the following formula [Fer17] :

$$w = \sqrt{\left(\left(\frac{r}{t}\right)^2 + \frac{l}{\pi t}\right)} - \frac{r}{t} \quad (13)$$

With :

- $l$  is the length of the booms coiled. In our configuration  $l = 14.14 \text{ m}$
- $r$  is the minimum coiling radius, or inner coiling radius
- $t$  is the thickness of the boom

### 3.4 Dimensions of the stowed membrane

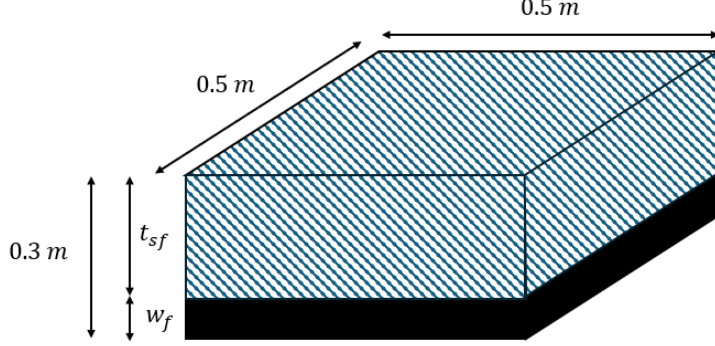


Figure 14: Sketch of the volume occupied by the membrane and the SBS in the stowed configuration

In order to quantify the flattened length  $w_f$  of the Bi-CTM booms that meets the requirements, we need to determine the thickness of the fully packaged three-layer sunshade by considering the geometric constrained of the stowed volume. From requirement  $R_1$ , the dimension of each membrane is  $20\text{ m} \times 20\text{ m}$ . From requirement  $R_2$ , the sunshade is comprised of three membrane layers, and, from requirement  $R_3$ , each membrane has a total thickness of  $5.01 \times 10^{-5}\text{ m}$  when fully deployed. This gives a total volume occupied by the membranes in the deployed configuration of approximately :  $V_m = 0.06\text{ m}^3$ .

Moreover, requirement  $R_7$  imposes a total stowed volume of dimensions  $0.5\text{ m} \times 0.5\text{ m} \times 0.3\text{ m}$ . Since no mass of the membrane is lost during folding or deployment, we can use the conservation of material to determine the stowed thickness. The stowed thickness  $t_{sf}$  is given by:

$$t_{sf} = \frac{V_m}{\text{Surface of the hub}} \quad (14)$$

Thus, the thickness of the fully stowed three-layer sunshade is approximately  $0.24\text{ m}$ , and we can determine a maximum length of the flattened Bi-CTM booms of  $0.06\text{ m}$

Hence, the following geometric constraint can be deduced from the stowed volume requirement:

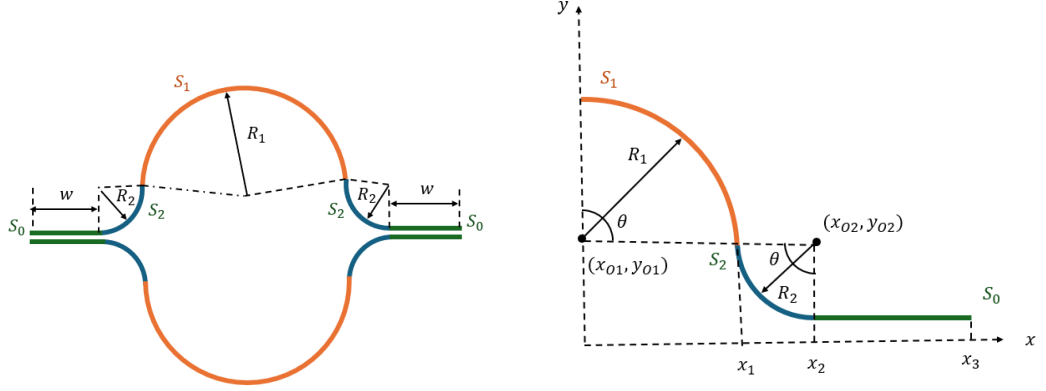
$$w_f \leq 0.06\text{ m} \quad (15)$$

### 3.5 Expression of the flattened length of the Bi-CTM booms

The Bi-CTM boom is composed of two booms, each consisting of five segments as depicted in Figure 20: two flat segments in green  $S_0$  of length  $w$ , two small curved segments  $S_2$  in blue and of radius  $R_2$ , and a long curved central segment  $S_1$  in orange and of radius  $R_1$ . For the top boom,  $S_2$  undergoes equal sense coiling, and  $S_1$  undergoes opposite sense coiling. In contrast, the bottom boom has  $S_2$  with opposite sense coiling and  $S_1$  with equal sense coiling. The two booms have the same minimum coiling radius  $r$ .

We can also express the flattened length  $w_f$  of the booms. From [CL14], we have the following expression of  $w_f$  as a function of  $R_1$ ,  $R_2$ ,  $\theta$  and  $w$  :

$$w_f = 2 \times (w + (R_1 + R_2)\theta) \quad (16)$$



(a) Cross sectional view and dimensions of the Bi-CTM boom when deployed

(b) Cross-sectional view showing the geometry of the Bi-CTM boom when deployed

Figure 15: Cross-sectional view showing the geometry and dimensions of the Bi-CTM boom when deployed

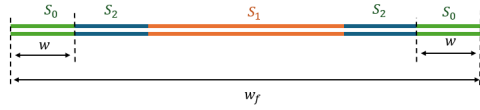


Figure 16: Cross sectional view of the Bi-CTM boom when flattened

The preliminary design parameter  $\theta$  indicates the angle between the axis ( $Oy$ ) and the segment  $O_1O_2$ . This parameter plays an important role in defining the ability of the Bi-CTM boom curved segments to flatten while remaining elastic. Let's give the expression of  $\cos(\theta)$ :

$$\cos(\theta) = \frac{y_{O2} - y_{O1}}{O_1O_2} = \frac{R_2 - y_{O1}}{R_1 + R_2}$$

We can derive an expression for  $w_f$  as a function of  $w$ ,  $R_1$ ,  $R_2$ , and  $y_{O1}$ .

$$w_f = 2 \times \left( w + (R_1 + R_2) \times \cos^{-1}\left(\frac{R_2 - y_{O1}}{R_1 + R_2}\right) \right) \quad (17)$$

Using the geometric constraint established in Equation 15, we can deduce additional constraints on the parameters  $R_1$ ,  $R_2$ , and  $w$ . These relationships will be essential in the geometric design of the booms.

### 3.6 Back-to-the envelope calculations

In this scenario, the sunshade must be designed to fit in the stowed configuration volume of  $0.5 \times 0.5 \times 0.24 \text{ m}^3$ . It is necessary to determine the parameters  $a$ ,  $b$ , and  $\alpha$  that satisfy the maximum allowable volume. As demonstrated in Section 2.4, the stowed length  $L_p$  and the packaged height  $H_p$  of the Miura-Ori configuration is given by:

$$L_p = b + 2n \times \left(\frac{L}{L_0}\right)a = b + 2n \times \cos(\alpha)a \quad \& \quad H_p = a \times \sin(\alpha)$$

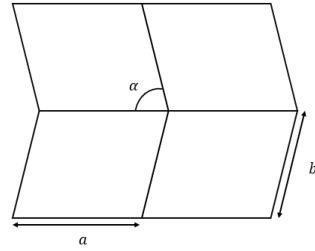


Figure 17: sketch of one unit cell of the membrane

Requirement R7 thus allows us to deduce a set of constraints on the parameters  $a$ ,  $b$ ,  $n$ , and  $\alpha$ , ensuring compliance with the prescribed design specifications.

$$b + 2n \times \cos(\alpha)a < 0.5 \quad (18)$$

And

$$a \times \sin(\alpha) < 0.5 \quad (19)$$

## **4. Geometry in the fully deployed case**

## 4.1 Second momentum of area of the Bi-CTM booms

A CTM boom comprises two circular segments and a flat segment, called web. The web is of length  $w$  and thickness  $t$ .  $R_1$  and  $R_2$  are the radii of the segment  $S_1$  and  $S_2$ , respectively, and  $O_1(x_{O1}, y_{O1})$  and  $O_2(x_{O2}, y_{O2})$  their centers. All segments have a thickness of  $t$ . We define  $\theta$  as the angle between the  $y$ -axis and the segment  $O_1O_2$ . Using Figure 20 and the literature [CL14], we can express formula of the moment of area about the  $x$ -axis and  $y$ -axis :

$$I_x = 4 \times \int_0^{x_M} \left( tR_1 \times \frac{(\sqrt{R_1^2 - x^2} + y_{O1})^2}{\sqrt{R_1^2 - x^2}} \right) dx + 4 \times \int_{x_M}^{x_{O2}} \left( tR_2 \times \frac{-(\sqrt{R_2^2 - (x - x_{O2})^2} + y_{O2})^2}{\sqrt{R_2^2 - (x - x_{O2})^2}} \right) dx \quad (20)$$

and

$$I_y = 4 \times \int_0^{x_M} \left( tR_1 \times \frac{x^2}{\sqrt{R_1^2 - x^2}} \right) dx + 4 \times \int_{x_M}^{x_{O2}} \left( tR_2 \times \frac{x^2}{\sqrt{R_2^2 - (x - x_{O2})^2}} \right) dx + 4 \int_{x_{O2}}^{x_{O2}+w} tx^2 dx \quad (21)$$

The moments of inertia,  $I_x$  and  $I_y$ , can be determined using the numerical integration in equations 30 and 31 or using an analytical integration [HK07]. The latter approach translates Equations 30 and 31 into :

$$\begin{aligned} I_x = & 2tR_1 \left( x_1 \sqrt{R_1^2 - x_1^2} + (R_1^2 + 2y_{O1}^2) \sin^{-1} \left( \frac{x_1}{R_1} \right) \right) + 2tR_2(x_2 - x_1) \left[ \sqrt{R_2^2 - (x_2 - x_1)^2} - 4R_2 \right] \\ & + 6tR_2^3 \sin^{-1} \left( \frac{x_2 - x_1}{R_2} \right) + 8tR_1x_1y_{O1} \end{aligned} \quad (22)$$

$$\begin{aligned} I_y = & 2tR_1 \left( R_1^2 \sin^{-1} \left( \frac{x_1}{R_1} \right) - x_1 \sqrt{R_1^2 - x_1^2} \right) + \frac{\beta t}{3}(x_3^3 + x_2^3) \\ & + 2tR_2 \left[ (3x_2 + x_1) \sqrt{R_2^2 - (x_2 - x_1)^2} - 4x_2R_2 \right] \\ & + 2tR_2(2x_2^2 + R_2^2) \sin^{-1} \left( \frac{x_2 - x_1}{x_1} \right) \end{aligned} \quad (23)$$

The coefficient  $\beta$  is the edge thickness coefficient and represents the different thickness along the the length. Initially  $\beta = 4$ , but this coefficient was revisited by Hakkak and Khoddam and is determined by the following formula :

$$\beta = 2 \times \frac{t_w}{t} \quad (24)$$

Where  $t_w$  it the thickness of the boom along the web and can be defined during the manufacturing process.

## 4.2 Impact of the material of the geometry of the Bi-CTM boom

It is essential to consider the material chosen for constructing the Bi-CTM booms in order to define some preliminary design parameter. As seen in section 3.2, the capacity of the material to flatten before coil is influenced by its elasticity and the geometry of the Bi-CTM boom. The selection of materials are based on the study conducted by Fernandez [Fer17]. This research focuses on the design of thin-shell rollable composite booms of length 6.83 m needed in the deployment of CubeSats' solar sails.

Thin-ply composites are studied to meet the strict thickness and density requirements while maximizing bending stiffness and minimizing mass. These composites exhibit ply thicknesses below 0.065 mm for unidirectional materials. The various composite materials evaluated in the study include :

- MR60H / PMT-F7 (CF)
- IM7 / RS-36 (CF)
- HTA40 / PMT-F7 (CF)

For the Bi-CTM boom configuration, it was shown that a two-ply [45PW/0] lay-up, utilizing HTA40/MR60H spread-tow carbon fiber materials, presents the optimal laminate configuration. This material will be considered in our design. The elastic modulus of the [45PW/0] laminate is  $E_{11} = 71.7$  GPa or  $71.7 \times 10^9$  N/m<sup>2</sup>

After selecting the material, it is crucial to consider the various limitations of the configuration. One of the essential consideration to take into account is the buckling of the designed CTM booms. The Bi-CTM mustn't buckle under applied loads while maintaining acceptable flattening and rolling strains. The behavior of the CTM boom will be similar to cantilever beams. Additionally, the design must maximize the principal moment of area.

To design the boom, we will adopt the configuration from the study and consider the following constraints:

- The subtended angle,  $\theta$ , must be within the range:

$$50^\circ \leq \theta \leq 90^\circ. \quad (25)$$

- The width of the web must satisfy:

$$3 \text{ mm} \leq w \leq 5 \text{ mm}. \quad (26)$$

Important shear stresses at the web increase with the reduction of the web size. However, larger web length may violate the stowage volume requirement.

- The maximum allowable strains in the axial and transverse directions  $\epsilon_{11}$  and  $\epsilon_{22}$  are constrained to 0.8%.
- If we consider a critical buckling load of  $P_{cr} = 3$  N and a support condition between fixed-free and pinned-pinned, the bending stiffness  $EI$  can be estimated given an effective length  $L_e$ . For our configuration, we consider that the effective length is the total length of the boom  $l$ , adjusted by a correction factor  $k$  to account for the support condition that is between fixed-free with a factor 1 and pinned-pinned with a factor of 2. In our case, we will consider a factor  $k = 1.19$ . By Euler's buckling equation, we can derive an expression for the bending stiffness:

$$EI = \frac{P_{cr}L_e^2}{\pi^2}. \quad (27)$$

### 4.3 Fundamental frequency of the Bi-CTM boom

We are treating the boom as a cantilever beam. The fundamental frequency of the cantilever beam can be written as :

$$f_0 = \frac{3.52}{2 \times \pi} \sqrt{\frac{EI}{ml^3}} \quad (28)$$

with  $f_0$  the fundamental frequency (in Hz), E the Young's modulus (in Pa), I the second momentum of area (in  $m^4$ ), m the mass (in kg) and l length (in m).

According to requirement  $R_8$ , the first mode frequency should be above 0.1 Hz. This condition leads to defining an inequation on the second moment of area of the CTM boom. Indeed :

$$f > f_0 \Rightarrow \frac{3.52}{2 \times \pi} \sqrt{\frac{EI}{ml^3}} > \frac{3.52}{2 \times \pi} \sqrt{\frac{EI_0}{ml^3}} \Rightarrow I > I_0$$

with

$$I_0 = \left(\frac{2\pi f_0}{3.52}\right)^2 \times \frac{ml^3}{E}$$

Hence, we have the following inequations :

$$I_x > I_0 \quad \& \quad I_y > I_0 \quad (29)$$

## **5. Design of the boom and the membrane**

## 5.1 Overall design of the Bi-CTM boom

From the section 4.2, we have seen that the critical constraints are linked to the subtended angle  $\theta$  and the width of the web  $w$ . These values are crucial in defining the validity of the CTM booms.

To simplify the design of the CTM booms, we will make some additional assumptions in order to focus only on two preliminary design parameters. Since we are interested in the influence of  $\theta$  and  $w$  on the boom design, we assume that  $R_1 = R_2$ . This simplification ensures that the only parameters affecting  $I_x$ ,  $I_y$ , and  $\epsilon_{22}$  are  $\theta$  and  $w$ .

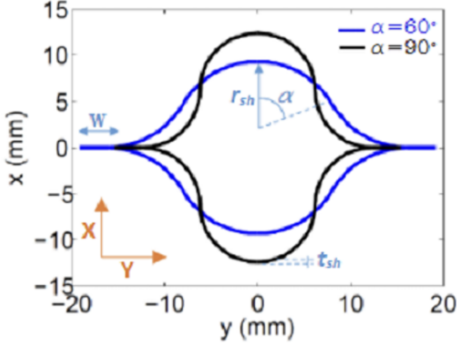


Figure 18: Cross sectional view dimensions of the Bi-CTM boom showing the influence off the parameters  $\theta$ ,  $w$  and  $R$  on the shape of the boom. In this case  $R = r_{sh}$  and  $\theta = \alpha$  [Fer17].

Given this assumption, we want to select values of  $w$  and  $\theta$  that satisfy the requirements. Specifically, the parameters must:

- Prevent buckling under applied forces.
- Ensure sufficient flattening strains and rolling strains.
- Maximize the principal moment of area.

## 5.2 Preliminary design parameters : coiling radius $r$ and thickness $t$

We are looking for a value of thickness  $t$  such that the outer radius  $r_o$  remains below the threshold 250 mm. To determine this value, we must also ensure that the other constraints are satisfied. Therefore, testing is required to identify a possible thickness  $t$ . For our design as shown in Figure 19,  $t < 0.9$  mm for an inner radius  $r = 55$  mm and  $t < 0.79$  mm for an inner radius  $r = 45$  mm. An increase in the inner radius translates into a decrease of the maximum thickness of the Bi-CTM booms.

In Section ??, we will propose a possible algorithm to determine a suitable thickness that meets all requirements.

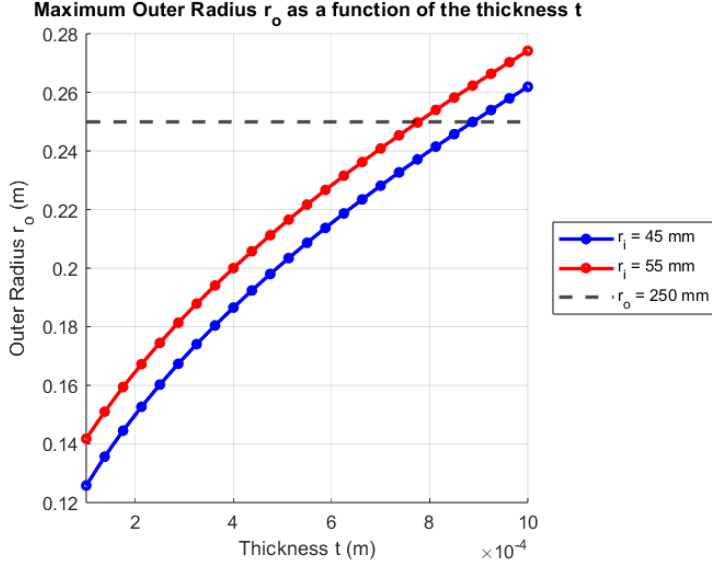


Figure 19: Evolution of the outer radius  $r_o$  with the thickness  $t$  of the boom with different values of inner radius  $r$

### 5.3 Preliminary parameters design choice : $\theta$

From Section 4.1, the following expression of  $I_x$  and  $I_y$  were given :

$$I_x = 2tR_1 \left( x_1 \sqrt{R_1^2 - x_1^2} + (R_1^2 + 2y_{O1}^2) \sin^{-1} \left( \frac{x_1}{R_1} \right) \right) + 2tR_2(x_2 - x_1) \left[ \sqrt{R_2^2 - (x_2 - x_1)^2} - 4R_2 \right] + 6tR_2^3 \sin^{-1} \left( \frac{x_2 - x_1}{R_2} \right) + 8tR_1x_1y_{O1} \quad (30)$$

$$I_y = 2tR_1 \left( R_1^2 \sin^{-1} \left( \frac{x_1}{R_1} \right) - x_1 \sqrt{R_1^2 - x_1^2} \right) + \frac{\beta t}{3} (x_3^3 + x_2^3) + 2tR_2 \left[ (3x_2 + x_1) \sqrt{R_2^2 - (x_2 - x_1)^2} - 4x_2R_2 \right] + 2tR_2(2x_2^2 + R_2^2) \sin^{-1} \left( \frac{x_2 - x_1}{x_1} \right) \quad (31)$$

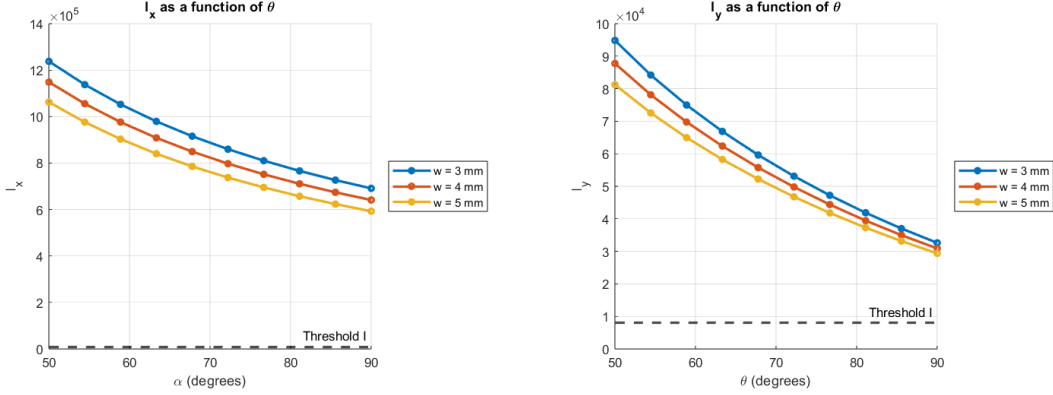
So if we consider  $R_1 = R_2 = R$  and  $y_{O1} = x_{O1} = 0$ , we have therefore:

$$I_x = 2tR^3 \sin(\theta) \times (R\theta - 4) + 4tR^3 \sin(\theta) \cos(\theta) + 6tR^2 \theta \quad (32)$$

$$I_y = 2tR^3 \sin(\theta) (1 - \cos(\theta)) + \frac{\beta t}{3} ((2R\sin(\theta) + w)^3 + (2R\sin(\theta))^3) + 16tR^3 \sin(\theta) (\cos(\theta) - 1) + 2tR^3 \theta (8\sin(\theta) + 1) \quad (33)$$

Since we avoid any buckling, we can establish the minimum required values for the moment of area about the  $x$ -axis and  $y$ -axis,  $I_x$  and  $I_y$ . Given that the effective length of the booms is  $k \times l$  m, we can express the minimum moment of area given the modulus of elasticity of the material  $E$ . From the results in Figure 20, there is no additional constraint on  $\theta$  for buckling.

$$I = \frac{P_{cr} k^2 l^2}{E \pi^2}, \quad (34)$$



(a) Evolution of the moment of area  $I_x$  about the  $x$ -axis with the subtended angle  $\theta$       (b) Evolution of the moment of area  $I_y$  about the  $y$ -axis with the subtended angle  $\theta$

Figure 20: Moments of area as functions of the subtended angle  $\theta$

One important observation is that the moment of area about the  $y$ -axis is decreasing when it should be increasing. Indeed, the larger the subtended angle, the greater the surface area along the  $y$ -axis. Moreover, the boom is more likely to buckle along the  $y$ -axis, as it is the smaller dimension and therefore closer to the threshold. Further investigation is needed to understand why the moment of area is decreasing. Moreover, If  $I_y$  is below the allowable threshold, the thickness  $t$  must be increased until the moment of area reaches the minimum required value.

#### 5.4 Validation of the preliminary design parameter : $\theta$

Figure 21 illustrates the maximum values of the subtended angle for different web width based on the maximum transverse strain. It shows that a subtended angle greater than  $80^\circ$  for a 3 mm web width exceed the maximum transverse strain for a flattening strain of 0.8%. The same way, the maximum transverse strain is reached for  $w = 5\text{mm}$  and  $\alpha = 72^\circ$ . Since we want to optimize the flattening width of the boom, we want the lower width possible. Hence the configuration chosen is  $w = 3\text{mm}$  and  $\alpha = 80^\circ$ .

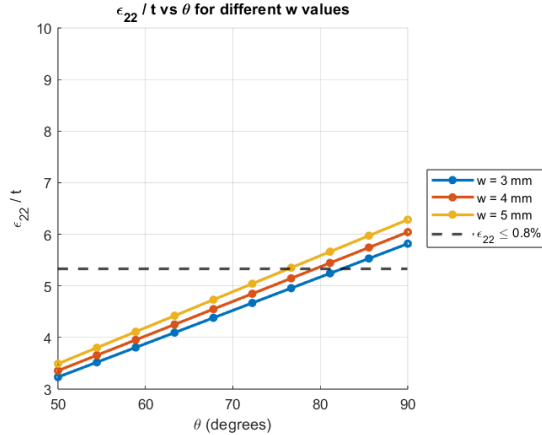


Figure 21: Transverse strain over the thickness for different web width as a function of the subtended angle  $\theta$

Moreover, if we are above the threshold, we must reduce  $\epsilon_{22}$ , hence the value of  $t$ . As long as we remain above the maximum value,  $t$  should continue to decrease.

## 5.5 Packaged dimensions of the membrane

Figures 22 and 23 illustrate the maximum values of the parameters  $a$  and  $b$  for the folding of the membrane, such that the stowed membrane meets the volume requirement. As the number of unit cells increases, the dimensions of each parallelogram decrease. As the angle  $\alpha$  increases, the values of  $a$  and  $b$  increase. One limitation of this representation is the assumption of zero thickness for the membrane, which make us unable to estimate the final thickness of the stowed membrane. The final thickness can potentially violate the stowed volume requirement. To improve the parameter selection ( $a$ ,  $b$  and  $n$ ), we could remove the zero-thickness assumption and quantify the folded membrane thickness.

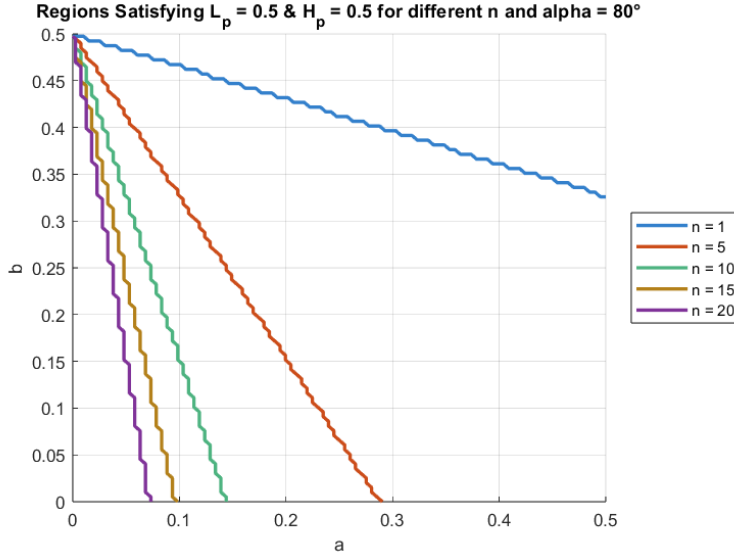


Figure 22: Regions (a,b) satisfying the volume constraints for different value of  $n$  and  $\alpha = 80^\circ$

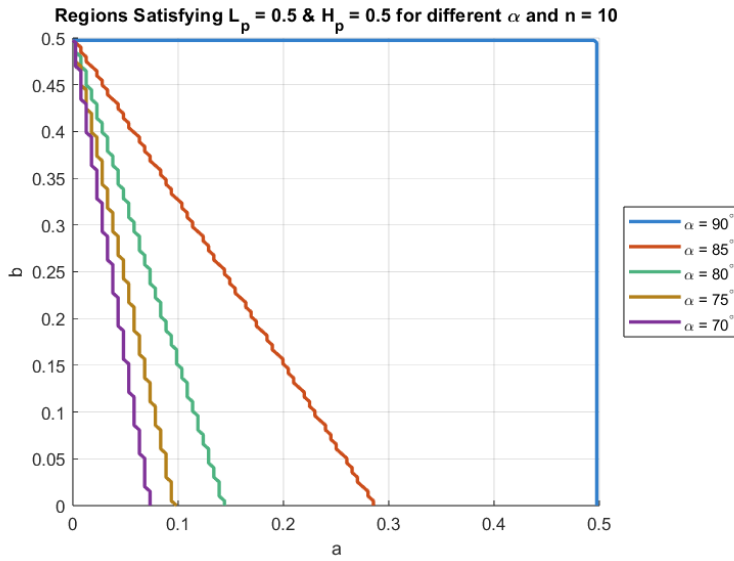


Figure 23: Regions (a,b) satisfying the volume constraints for different value of  $\alpha$  and  $n = 10$

## 5.6 Algorithm

We have seen that, in order to meet the requirements, we can change a single parameter when considering the optimal geometry of the Bi-CTM booms, which means a web length  $w = 3$  mm: the parameter  $t$ . Moreover, we have seen that while  $I_y$  is under the threshold, we need to increase  $t$ , and while  $\epsilon_{22}$  is above the threshold, we need to decrease  $t$ . Hence, the most important quantifiable values used to define the acceptable configuration are controlled by  $t$ . Therefore, we can write an algorithm to find the convergent value of  $t$  that meets these two requirements at the same time.

---

**Algorithm 1** Pseudocode for preliminary design parameters definition

---

```

1: Input: Initial coiling radius  $r$ , number of booms  $n$ , web width  $w$ 
2: Output: The thickness of the booms  $t$ 
3: calculate  $\max(r_o)$ ,
4: calculate  $t(\max(r_o))$  using Eq. (12)
5:  $t \leftarrow t(\max(r_o))$ 
6: calculate  $I_y$  and  $\epsilon_{22}$  using Eq. (10), (23)
7: while  $I_y <$  Threshold buckling or  $\epsilon_{22} > 0.8\%$  do
8:   if  $r_o(t) > \max(r_o)$  then
9:     Error: Exceeded allowable limit
10:    exit
11:   else if  $I_y <$  Threshold buckling then
12:     Increase  $t$ 
13:   else if  $\epsilon_{22} > 0.8\%$  then
14:     Decrease  $t$ 
15:   else
16:     break
17:   end if
18:   Recalculate  $I_y$  and  $\epsilon_{22}$  based on new  $t$ 
19: end while
20: Print "Converged thickness:",  $t$ 
```

---

## **6. MATLAB Code**

Listing 1: MATLAB Code for the maximum outer radius  $r_o$  as a function of the thickness  $t$

```

1 clc; clear; close all;
2
3 l = 14.14;
4 mu = 0.25;
5 r = [0.045, 0.055];
6 t = linspace(0.0001, 0.001, 25);
7 r_o = zeros(length(r), length(t));
8
9 for i = 1:length(r)
10    for j = 1:length(t)
11        t_t = 8 * t(j) * (1 + mu);
12        r_o(i, j) = r(i) + t_t * sqrt((r(i) / t_t)^2 + 1 / (pi * t_t));
13    end
14 end
15
16 figure;
17 hold on;
18 plot(t, r_o(1, :), 'bo-', 'LineWidth', 2, 'MarkerSize', 4);
19 plot(t, r_o(2, :), 'ro-', 'LineWidth', 2, 'MarkerSize', 4);
20 yline(0.25, 'k--', 'LineWidth', 2);
21 legend({'r_o=45mm', 'r_o=55mm', 'r_o=250mm'}, 'Location', 'eastoutside');
22 xlabel('Thickness t (m)');
23 xlim([0.1*10^(-3) 1*10^(-3)]);
24 ylabel('Outer Radius r_o (m)');
25 title('Maximum Outer Radius r_o as a function of the thickness t');
26 grid on;
27 hold off;

```

Listing 2: MATLAB Code for  $I_x$  and  $I_y$  as functions of  $\theta$  for different  $w$

```

1 %Constants
2 l = 14.14;
3 P_cr = 3;
4 E = 71.7e9;
5 t = 0.00015;
6 I_threshold = (P_cr * 1.19 ^2* l^2*10^9) / (t*E* pi^2);
7 beta = 4;
8 w = [0.003, 0.004, 0.005];
9 alpha = linspace(50, 90, 10);
10
11 % Initialize I_x and I_y
12 I_x = zeros(length(w), length(alpha));
13 I_y = zeros(length(w), length(alpha));
14
15
16 for i = 1:length(w)
17    for j = 1:length(alpha)
18        theta = deg2rad(alpha(j));
19        R = (0.06 - 2*w(i))/(4*theta);
20        Ix = 2*t*R^3*sin(theta)*(R*theta - 4) + 4*t*R^3*sin(theta)*cos(theta) + 6*t*R
21            ^2*theta;
22        Iy = 2*t*R^3*(theta - sin(theta)*cos(theta)) + (beta * t / 3) * ((2*R*sin(
23            theta) + w(i))^3 + (2*R*sin(theta))^3) + 2*t*R^3*sin(theta)*(7*cos(theta) -
24            4) + 2*t*R^3*theta*(8*sin(theta) + 1);
25        I_x(i, j) = Ix*10^9/t;
26        I_y(i, j) = Iy*10^9/t;
27    end
28 end
29
30 % Plot I_x
31 figure;
32 hold on;
33 for i = 1:length(w)
34    plot(alpha, I_x(i, :), 'o-', 'LineWidth', 2, 'MarkerSize', 4);
35 end
36 yline(I_threshold, 'k--', 'LineWidth', 2, 'Label', 'Threshold I');
37 legend({'w=3mm', 'w=4mm', 'w=5mm'}, 'Location', 'eastoutside');
38 xlabel('alpha (degrees)');

```

```

37 ylabel('I_x');
38 title('I_x as a function of \alpha');
39 grid on;
40 hold off;
41
42 % Plot I_y
43 figure;
44 hold on;
45 for i = 1:length(w)
46 plot(alpha, I_y(i, :), 'o-', 'LineWidth', 2, 'MarkerSize', 4);
47 end
48 yline(I_threshold, '--k', 'LineWidth', 2, 'Label', 'Threshold_I');
49 legend({'w=3mm', 'w=4mm', 'w=5mm'}, 'Location', 'eastoutside');
50 xlabel('\theta(degrees)');
51 ylabel('I_y');
52 title('I_y as a function of \theta');
53 grid on;
54 hold off;

```

Listing 3: MATLAB Code for  $\epsilon_{22}/t$  as a function of  $\theta$  for different  $w$

```

1 t = 0.00015;
2 theta = linspace(50*pi/180, pi/2, 10);
3 w = [0.003, 0.004, 0.005];
4 threshold = 0.8/ 0.15;
5 figure;
6 hold on;
7 for i = 1:length(w)
8 R = (0.06-2*w(i)) ./ (4*theta);
9 epsilon_22_t = 100 ./ (2*R*1000);
10 plot(theta * (180/pi), epsilon_22_t, 'o-', 'LineWidth', 2, 'MarkerSize', 4);
11 end
12 yline(threshold, '--k', 'LineWidth', 2);
13 legend({'w=3mm', 'w=4mm', 'w=5mm', '\epsilon_{22} \leq 0.8%'}, 'Location', 'eastoutside');
14 xlabel('\theta(degrees)');
15 ylabel('\epsilon_{22}/t');
16 ylim([3 10]);
17 title('\epsilon_{22}/t vs \theta for different w values');
18 grid on;
19 hold off;

```

Listing 4: Estimation of a and b based on the back-to-the envelope calculations

```

1 clc; clear; close all;
2
3 a = linspace(0, 0.5, 100);
4 b = linspace(0, 0.5, 100);
5 alpha = deg2rad([90, 85, 80, 75, 70]);
6
7 colors = {[0.2 0.5 0.8],
8 [0.8 0.3 0.1],
9 [0.3 0.7 0.5],
10 [0.7 0.5 0.1],
11 [0.5 0.2 0.6]};
12
13 [A, B] = meshgrid(a, b);
14
15 figure;
16 hold on;
17 grid on;
18 xlabel('a');
19 ylabel('b');
20 title('Regions Satisfying L_p=0.5 & H_p=0.5 for different \alpha and n=10');
21 xlim([0 0.5]);
22 ylim([0 0.5]);
23 legend_labels = cell(length(alpha), 1);
24 n = 10;
25 for i = 1:length(alpha)
26 L_p = B + 2 * n * cos(alpha(i)) .* A;

```

```

27     H_p = A .* sin(alpha(i));
28     valid_region = (L_p < 0.5) & (H_p < 0.5);
29     contour(A, B, valid_region, [0.5 0.5], 'Color', colors{i}, 'LineWidth', 2);
30     legend_labels{i} = sprintf('\\alpha=%d^\\circ', round(rad2deg(alpha(i))));
31 end
32 legend(legend_labels, 'Location', 'eastoutside');
33 hold off;
34
35 figure;
36 hold on;
37 grid on;
38 xlabel('a');
39 ylabel('b');
40 title('Regions Satisfying L_p=0.5 & H_p=0.5 for different n and alpha=80');
41 xlim([0 0.5]);
42 ylim([0 0.5]);
43 legend_labels = cell(length(colors), 1);
44 n = [1, 5, 10, 15, 20];
45 alpha = deg2rad(80);
46 for i = 1:length(n)
47     L_p = B + 2 * n(i) * cos(alpha) .* A;
48     H_p = A .* sin(alpha);
49     valid_region = (L_p < 0.5) & (H_p < 0.5);
50     contour(A, B, valid_region, [0.5 0.5], 'Color', colors{i}, 'LineWidth', 2);
51     legend_labels{i} = sprintf('n=%d', n(i));
52 end
53 legend(legend_labels, 'Location', 'eastoutside');
54 hold off;

```

# References

- [Cen21] DLR German Aerospace Center. Setting the solar sail, 2021. Accessed: Feb. 23, 2025.
- [CL14] ZhongYi Chu and YiAn Lei. Design theory and dynamic analysis of a deployable boom. *Mechanism and Machine Theory*, 71:126–141, 2014.
- [Fer17] Juan M Fernandez. Advanced deployable shell-based composite booms for small satellite structural applications including solar sails. In *International Symposium on Solar Sailing 2017*, number NF1676L-25486, 2017.
- [GP92] Simon D Guest and Sergio Pellegrino. Inextensional wrapping of flat membranes. In *Proceedings of the first international seminar on structural morphology*, volume 25. University of Montpellier, 1992.
- [HK07] F Hakkak and Shahin Khoddam. On calculation of preliminary design parameters for lenticular booms. *Proceedings of the Institution of Mechanical Engineers, Part G: Journal of Aerospace Engineering*, 221(3):377–384, 2007.
- [MP20] Koryo Miura and Sergio Pellegrino. *Forms and concepts for lightweight structures*. Cambridge University Press, 2020.
- [SH21] Marco Straubel and Christian Hühne. Ctm boom deployment mechanism with integrated boom root deployment for increased stiffness of the boom-to-spacecraft interface. 2021.
- [Wil21] William K Wilkie. Overview of the nasa advanced composite solar sail system (acs3) technology demonstration project. In *AIAA Scitech 2021 Forum*, page 1260, 2021.